Few-body calculations of proton-^{6,8}He scattering

J. S. Al-Khalili and J. A. Tostevin
Department of Physics, School of Physical Sciences, University of Surrey, Guildford, Surrey, GU2 5XH, United Kingdom
(Received 18 November 1997)

We present a theoretical analysis of recently published experimental data for the elastic scattering of protons from the helium isotopes ^{6}He and ^{8}He at energies near 700 MeV per nucleon. The analysis treats the few-body degrees of freedom of these light neutron-rich nuclei explicitly and is developed in terms of three- and five-body wave functions for ^{6}He and ^{8}He, respectively. Comparisons of calculations with the data show that the sizes of the He nuclei consistent with such an analysis are larger by about 0.2 fm than those deduced from a more approximate procedure in which the structure of the weakly bound nuclei enters only through an assumed nuclear matter density. [S0556-2813(98)06504-2]

PACS number(s): 25.10.+s, 24.10.Eq, 24.50.+g, 25.40.Cm

I. INTRODUCTION

In a recent paper [1], experimental data for the elastic scattering of protons from the helium isotopes ^{4}He, ^{6}He, and ^{8}He, at energies near 700 MeV/nucleon, have been presented and compared. These data were also used there to estimate the sizes of the ^{6}He and ^{8}He nuclei by the use of an approximation to Glauber's theory [2] of composite particle scattering and using an assumed (point nucleon) one-body density for each of these light nuclei. Within this approximate model the authors fitted the measured differential cross sections for each He isotope independently and observed considerable insensitivity in their fit to the precise parametrization assumed for the one-body density, other than to its root-mean-squared (rms) matter radius. The authors concluded that the nuclear rms matter radii so extracted were therefore essentially model independent and quoted deduced radii for ^{6}He and ^{8}He of 2.30 ± 0.07 fm and 2.45 ± 0.07 fm, respectively, with small errors.

The deduced size for ^{6}He in particular is smaller than one would expect based on other empirical information. For instance, this ^{6}He radius is smaller than that normally assumed (2.44 fm) for ^{6}Li, derived from the measured rms charge radius from electron scattering [3] by unfolding the charge form factors of the nucleons. On the other hand, the high-energy total interaction cross section measurements of Tanihata and co-workers obtain a cross section for ^{6}He+^{12}C [4] (722 ± 5 mb) which is significantly larger than that for ^{6}Li+^{12}C [5] (688 ± 10 mb). These data have been shown, in two quite different approaches [6,7], to be consistent with a ^{6}He rms matter radius of order 2.52–2.57 fm. That the Borromean ^{6}He ground state, with its two neutron separation energy of only 0.97 MeV, is also the isobaric analog state of the $T=1$ 0^+ state at 3.56 MeV excitation in ^{6}Li, would also lead one to anticipate that the ground-state configuration would be more spatially extended in the case of ^{6}He.

In this paper, unlike the nuclear-density-based reaction analysis of Alkhazov *et al.* [1], we calculate the proton elastic scattering from the ^{A}He systems in terms of their few-body wave functions. We will *not* therefore make the additional approximations, involving the neglect of few-body and other correlations, needed to reduce the dependence of the scattering on the projectile structure simply to that of an assumed nuclear one-body density. It was already shown in Refs. [8,9,6], there in the context of total reaction cross section calculations, that an explicit treatment of the correlations present in the few-body wave functions of such nuclei is of considerable quantitative importance. The few-body degrees of freedom, when treated accurately, were shown to increase the transparency of the nuclear collision at large impact parameters resulting in a smaller calculated reaction cross section and hence in larger deduced nuclear sizes in comparisons with data. The purpose of this paper is to clarify the importance of these few-body correlations for calculations of elastic scattering observables, and hence for the sizes of the He isotopes suggested from comparisons with the experimental data of Ref. [1].

II. THEORETICAL BACKGROUND

According to Glauber's multiple-scattering theory the elastic amplitude for the scattering of a proton from a composite nucleus of mass A can be written as an integral over the proton impact parameter plane as [2]

$$f(\boldsymbol{q})=\frac{ik}{2\pi}\int d^2\boldsymbol{b}e^{i\boldsymbol{q}\cdot\boldsymbol{b}}[1-\mathcal{S}_A(b)]. \tag{1}$$

Here k is the proton's incident wave number in the center-of-mass (c.m.) frame and q is the momentum transfer in the scattering. The elastic S matrix, as a function of the proton-target c.m. impact parameter b, is

$$\mathcal{S}_A(b)=\left\langle \Phi_A\left|\prod_{j=1}^{A} S_{pj}(b_j)\right|\Phi_A\right\rangle, \tag{2}$$

where the label j runs over each nucleon in the composite target, with ground-state wave function Φ_A. Each pairwise nucleon-nucleon (NN) scattering operator (S matrix) is denoted by $S_{pj}(b_j)=1-\Gamma_{pj}(b_j)$ where b_j is the impact parameter of the incident proton relative to target nucleon j. The j label on Γ_{pj} also identifies the use of the pn or pp profile function, the two-dimensional transform of the free NN scattering amplitudes

 © 1998 The American Physical Society

$$\Gamma_{pj}(b_j)=\frac{1}{2\pi ik}\int d^2\boldsymbol{q}e^{-i\boldsymbol{q}\cdot\boldsymbol{b}_j}f_{pj}(q). \tag{3}$$

These profile functions are parametrized, as is usual, according to

$$\Gamma_{pj}(b)=\frac{\sigma_{pj}}{4i\pi\beta_{pj}}(\alpha_{pj}+i)\exp(-b^2/2\beta_{pj}) \quad (j=p,n), \tag{4}$$

where σ_{pp} and σ_{pn} are the pp and pn total cross sections. The α_{pj} are the ratios of the real to imaginary parts if the forward scattering NN amplitudes and the β_{pj} are the range parameters. All parameters are deduced, e.g. [10,11], from fits to free pp and pn scattering data.

In the present analysis, where the proton scattering experiments were actually performed in inverse kinematics, then $|\Phi_A\rangle$ is to be identified with the many-body ground state of the projectile. It must be stressed that the composite nucleus S matrix, $\mathcal{S}_A(b)$ in Eq. (2), is a many-body matrix element of the projectile ground-state many-body density $|\Phi_A|^2$ and, without considerable additional approximation, $\mathcal{S}_A(b)$ has no simple relationship with the projectile one-body density $\rho_A(r)$. In the work of Ref. [1], such ground-state many-body densities are in fact taken as products of one-body densities for ^{4}He, and for the neutron-rich ^{6}He and ^{8}He systems. While such an approximation is arguable for the compact ^{4}He system, where all nucleons share a common volume of space, the known strong spatial correlations of the nucleons in ^{6}He and ^{8}He, into an α particle core and a valence neutron halo/skin component, makes such an (uncorrelated) factorization of doubtful validity.

For such nuclei, and other halo nuclei, which have a well-defined cluster decomposition, an alternative few-body structure description is more appropriate. In such cases the A-nucleon composite nucleus is considered as an effective n-cluster system. For halo nuclei the expectation, due to the weak valence nucleon binding, is that the core polarization effects are small. Such an approximation is expected to be particularly good for the He isotopes in which the core fragment is the α particle [12]. Such nuclei have therefore been modeled successfully as an inert core with $n-1$ loosely bound interacting valence nucleons. The many-body wave function in this case is expressed as a product of the intrinsic wave function of the core, of mass A_c, and an n-body wave function which describes the relative motion of all of the clusters.

When included in the elastic scattering S matrix, Eq. (2), the n-cluster variant of the A-body matrix element then reads

$$\begin{aligned}\mathcal{S}_A^{(n)}(b)&=\left\langle \Phi_{A_c}\psi_{\rm rel}^{(n)}\left|\prod_{j=1}^{A}S_{pj}(b_j)\right|\Phi_{A_c}\psi_{\rm rel}^{(n)}\right\rangle\\&=\left\langle \psi_{\rm rel}^{(n)}\left|\mathcal{S}_{A_c}(b_c)\prod_{j=1}^{n-1}S_{pj}(b_j)\right|\psi_{\rm rel}^{(n)}\right\rangle.\end{aligned} \tag{5}$$

Here $\psi_{\rm rel}^{(n)}$ denotes the n-cluster relative motion wave function, expressed in suitable coordinates, and Φ_{A_c} is the core wave function. Also, $\mathcal{S}_{A_c}(b_c)$ is the S matrix for elastic proton scattering from the free composite core nucleus at the same incident energy per nucleon. This is given by Eq. (2), but now with $A=A_c$.

Within this cluster picture a hierarchical structure therefore develops in which the scattering of the n-cluster composite nucleus is entirely determined by the scattering properties (S matrices) of its n constituent clusters and by their assumed relative motion wave function $\psi_{\rm rel}^{(n)}$. Given these inputs, and noting that the core and nucleon scattering inputs $\mathcal{S}_{A_c}$ and S_{pj} can be assessed by comparisons with quite independent data, any given few-body wave-function model $\psi_{\rm rel}^{(n)}$ leads to a specific prediction for the scattering of the projectile without free parameters. We reiterate that, as for the original A-body scattering matrix element $\mathcal{S}_A(b)$, the n-cluster matrix element $\mathcal{S}_A^{(n)}(b)$ remains a many-body matrix element, now of the projectile's few-body density $|\psi_{\rm rel}^{(n)}|^2$ and has no simple correspondence with the projectile's one-body density $\rho_A(r)$.

In the approach outlined above, the calculation of the elastic S matrices for the ^{6}He and ^{8}He composites are developed from those of their constituent clusters at the same incident energy per nucleon. It follows that a necessary input for the $A=6$ and $A=8$ systems is the S matrix for the proton-α particle core scattering $\mathcal{S}_4(b)$. This, in turn, should be consistent with the available $p+^4$He scattering data.

A. Treatment of the p+^{4}He scattering

$\mathcal{S}_4$ is computed here according to Eq. (2) as

$$\begin{aligned}\mathcal{S}_4(b)&=\left\langle \Phi_4\left|\prod_{j=1}^{4}S_{\rm NN}(b_j)\right|\Phi_4\right\rangle\\&=\int\prod_{j=1}^{4}[d\boldsymbol{r}_jS_{\rm NN}(b_j)]|\Phi_4(\boldsymbol{r}_1,\boldsymbol{r}_2,\boldsymbol{r}_3,\boldsymbol{r}_4)|^2,\end{aligned} \tag{6}$$

where, for the $T=0$ α particle, we set $S_{\rm NN}(b_j)=1-\Gamma_{\rm NN}(b_j)$ with $\Gamma_{\rm NN}$ the transform of the isospin average of the elementary pn and pp amplitudes. The four-body α particle density is taken to be of the simple form

$$|\Phi_4(\boldsymbol{r}_1,\boldsymbol{r}_2,\boldsymbol{r}_3,\boldsymbol{r}_4)|^2=\mathcal{N}(r_0)\prod_{j=1}^{4}|\phi(r_j)|^2\delta\left(\sum_{i=1}^{4}\boldsymbol{r}_i\right), \tag{7}$$

and thus includes explicitly only the c.m. correlations of the nucleons within the α particle. Here $\mathcal{N}(r_0)$ is an appropriate normalization constant and, assuming that $\phi(r)$ is the nodeless s-state oscillator function, then

$$|\phi(r_j)|^2=(\sqrt{\pi}r_0)^{-3}\exp(-r_j^2/r_0^2). \tag{8}$$

The value of r_0 will be chosen so that the α particle rms matter radius $\langle r^2\rangle_4^{1/2}$ is 1.49 fm which is consistent with the rms charge radius deduced from electron scattering [3] after folding in the nucleon charge form factors. The calculational procedure used to compute Eq. (6) is discussed in the following sections.

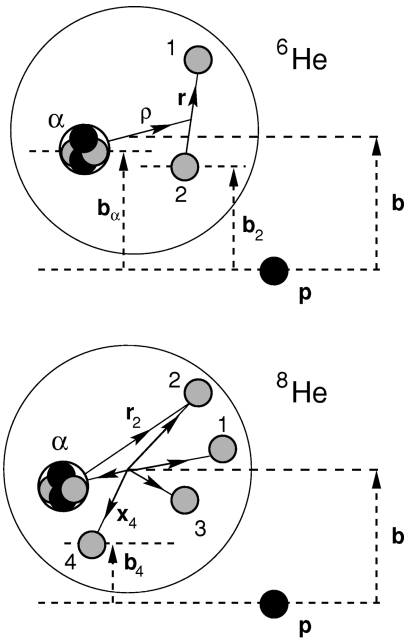

FIG. 1. Schematic representation of the few-body models and coordinate systems used for the description of the four-body $p+{}^6$He (upper) and six-body $p+{}^8$He (lower) scattering systems. The impact parameter of the projectile's center of mass and of each constituent cluster is also indicated.

B. Treatment of the $p+{}^6$He scattering

From Eq. (5), the elastic S matrix for $p+{}^6$He scattering, within the $\alpha+n+n$ three-body model of ^{6}He, is written

$$\mathcal{S}_6^{(3)}(b)=\langle\psi_{\rm rel}^{(3)}|\mathcal{S}_4(b_\alpha)S_n(b_1)S_n(b_2)|\psi_{\rm rel}^{(3)}\rangle, \tag{9}$$

where $S_n(b_i)$ and $\mathcal{S}_4(b_\alpha)$ are the S matrices for free pn and $p\alpha$ scattering discussed above. The only new input required here is the three-body ground-state wave function for ^{6}He, $\psi_{\rm rel}^{(3)}$, which can be chosen from a selection of realistic (Faddeev) wave-function models such as are tabulated in Ref. [9]. These wave functions all assume an inert α particle core but take fully into account the effects of correlations between the two valence neutrons and with the core. For this reason $\psi_{\rm rel}^{(3)}$ does not factorize as a product of single-particle wave functions for each neutron, but takes the general form [13]

$$\psi_{\rm rel}^{(3)}(\boldsymbol{\rho},\boldsymbol{r})=\sum_{\ell\lambda LS}\phi_{\ell\lambda LS}(\rho,r)[[Y_\ell(\hat{\boldsymbol{\rho}})\otimes Y_\lambda(\hat{\boldsymbol{r}})]_L \otimes[\chi_{\frac12}(1)\otimes\chi_{\frac12}(2)]_S]_{J=0,M=0}. \tag{10}$$

Here $\boldsymbol{\rho}$ and $\boldsymbol{r}$ are the Jacobi coordinates defined in Fig. 1 and the relative orbital angular momenta ℓ and λ refer to the coordinates $\boldsymbol{\rho}$ and $\boldsymbol{r}$, respectively. The $\chi_{1/2}(i)$ are the neutron spinors. Since the two neutron spins can couple only to total spin 0 or 1 the requirement $L=S$ restricts the wave function to s- and p-wave total orbital angular momentum components. Full details of the angular momentum structure of the three-body wave functions used can be found in [13].

$\mathcal{S}_6^{(3)}(b)$ is thus obtained upon integrating over the two internal vector coordinates of the three-body wave function, i.e.,

$$\mathcal{S}_6^{(3)}(b)=\int d\boldsymbol{\rho}\int d\boldsymbol{r}\langle|\psi_{\rm rel}^{(3)}(\boldsymbol{\rho},\boldsymbol{r})|^2\rangle_{\rm spin}\mathcal{S}_4(b_\alpha)S_n(b_1)S_n(b_2), \tag{11}$$

where $b_\alpha=|\boldsymbol{b}-\boldsymbol{\sigma}/3|$, $b_i=|\boldsymbol{b}+2\boldsymbol{\sigma}/3\pm\boldsymbol{s}/2|$, and $\boldsymbol{\sigma}$ and $\boldsymbol{s}$ are the projections of the vectors $\boldsymbol{\rho}$ and $\boldsymbol{r}$ on to the plane perpendicular to the projectile incident momentum. The $\langle\ldots\rangle_{\rm spin}$ notation indicates an integration over the spin degrees of freedom of the two neutrons. Full details of the structure of the calculation of Eq. (11) which results when using the three-body wave functions given in Eq. (10) can be found in [13].

C. Treatment of the $p+{}^8$He scattering

Similarly the elastic S matrix for $p+{}^8$He scattering, within an $\alpha+4n$ description of ^{8}He, is

$$\mathcal{S}_8^{(5)}(b)=\langle\psi_{\rm rel}^{(5)}|\mathcal{S}_4(b_\alpha)S_n(b_1)S_n(b_2)S_n(b_3)S_n(b_4)|\psi_{\rm rel}^{(5)}\rangle, \tag{12}$$

where the constituent $S_n(b_i)$ and $\mathcal{S}_4(b_\alpha)$ are precisely as for the ^{6}He case. We make use here only of the cluster orbital shell-model approximation (COSMA) wave function for $\psi_{\rm rel}^{(5)}$ [14]. This provides a convenient expression for the spin-integrated four-neutron correlation function entering Eq. (12). It includes explicitly the cluster correlations and also those correlations associated with the antisymmetrization of the four valence neutrons, amongst themselves, each in an assumed $p_{3/2}$ orbital with respect to the α core. Explicitly, from Eq. (6) of Ref. [14],

$$\langle|\psi_{\rm rel}^{(5)}(\boldsymbol{r}_1,\boldsymbol{r}_2,\boldsymbol{r}_3,\boldsymbol{r}_4)|^2\rangle_{\rm spin}=\left[\prod_{i=1}^4\frac{|\phi(r_i)|^2}{4\pi}\right]\mathcal{A}(1,2,3,4), \tag{13}$$

where ϕ is a nodeless p-wave radial wave function. Here the vectors $\boldsymbol{r}_i$ are the positions of the four neutrons relative to the α particle core (see Fig. 1). The angular correlations are given by

$$\mathcal{A}(1,2,3,4)=\frac34(s_{12}^2s_{34}^2+s_{13}^2s_{24}^2+s_{14}^2s_{23}^2), \tag{14}$$

where $s_{ij}^2=1-(\hat{\boldsymbol{r}}_i\cdot\hat{\boldsymbol{r}}_j)^2$ is the square of the sine of the angle between vectors $\boldsymbol{r}_i$ and $\boldsymbol{r}_j$. The calculational procedure used is outlined in the following section.

III. CALCULATIONAL DETAILS AND RESULTS

To calculate the elastic-scattering amplitudes and differential cross sections for the $p+{}^A$He systems ($A=4,6,8$) we need to evaluate the few-body elastic S matrices $\mathcal{S}_4$, $\mathcal{S}_6^{(3)}$, and $\mathcal{S}_8^{(5)}$, defined in Eqs. (6), (11), and (12), respectively. We also require the pn nucleon-nucleon scattering S matrix S_n, which enters Eqs. (11) and (12) and the isospin averaged nucleon-nucleon amplitude $S_{\rm NN}$ which enters the Eq. (6).

The elementary NN scattering parameters used in Eq. (4)

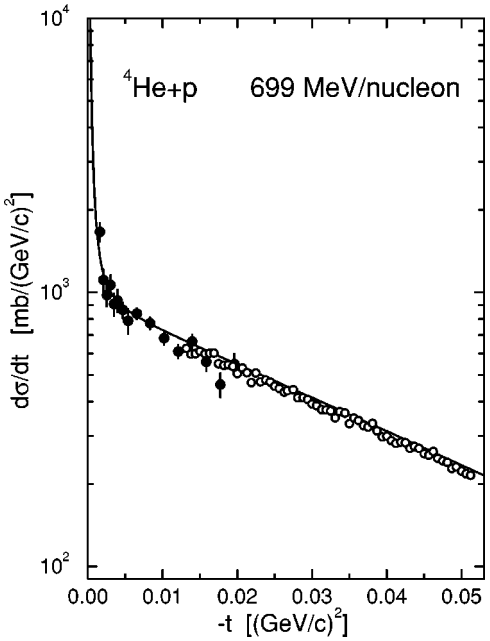

FIG. 2. Calculated and experimental $p+^4$He elastic differential cross section angular distribution as a function of the square of the four-momentum transfer ($q^2=-t$) at 699 MeV per nucleon. The data are from Refs. [1] (solid points) and [15] (open points).

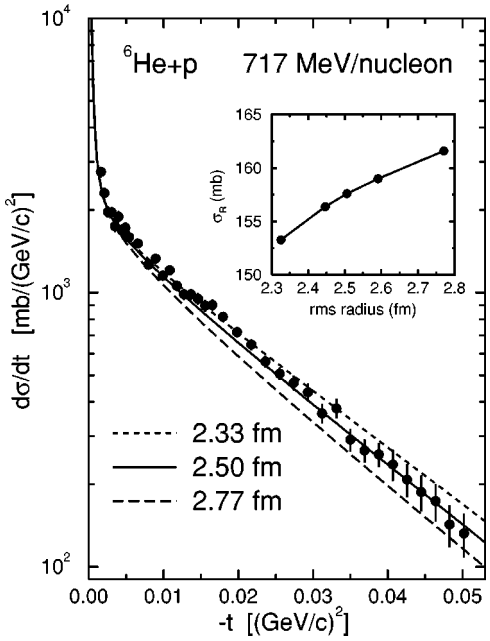

FIG. 3. Calculated and experimental $p+^6$He elastic differential cross section angular distribution as a function of the square of the four-momentum transfer ($q^2=-t$) at 717 MeV per nucleon. The calculations use the different three-body ^{6}He wave functions discussed in the text and which generate ^{6}He nuclei with the rms matter radii indicated. The inset shows the predicted total reaction cross sections as a function of the rms matter radius. The data are from Ref. [1].

were obtained by interpolating the parameter values given in Table I of Ref. [10] to 700 MeV proton energy. Only the central terms of the NN amplitude are retained The values used in this analysis were $\sigma_{pp}=44.3$ mb, $\sigma_{pn}=37.7$ mb, $\alpha_{pp}=0.1$, $\alpha_{pn}=-0.38$, $\beta_{pp}=0.16$ fm^2, and $\beta_{pn}=0.2$ fm^2. These parameters were kept fixed throughout our analysis and used for all the He isotopes, without adjustment. No attempt has been made to improve calculations by parameter variation since an aim is to assess the basic consistency of our hierarchical few-body picture for all three He systems. In the approach followed here, these systems are not independent but have common theoretical and derived inputs. In all calculations the Coulomb interaction is included and is assumed to act at the center of mass of the composite projectile [2].

A. Calculations for ^{4}He

For both the $p+^4$He and $p+^8$He systems the multidimensional integrals involved in Eqs. (6) and (12) were computed using random sampling (Monte Carlo) integration methods. For the $p+^4$He system, and at each value of the ^{4}He c.m. impact parameter b, the calculations sampled at random the position vectors $\boldsymbol{r}_1$, $\boldsymbol{r}_2$ and $\boldsymbol{r}_3$ of three of the nucleons with respect to the ^{4}He c.m., from which $\boldsymbol{r}_4$ was then computed to be consistent with the center-of-mass constraint. In each such four-nucleon spatial configuration the $|\phi(r_j)|^2$ were evaluated, the constituent b_j calculated, and the $S_{\rm NN}(b_j)$ were then interpolated from a precalculated lookup table. The value $r_0=1.405$ fm was used in Eq. (8) which calculated an alpha particle rms matter radius $\langle r^2\rangle_4^{1/2}=3r_0/2\sqrt{2}=1.49$ fm.

The results for the $p+^4$He scattering angular distribution at 699 MeV are shown in Fig. 2. Following the presentation of the experimental data of Ref. [1], we calculate the differential cross section as a function of the square of the four momentum transfer ($q^2=-t$). The data are from Refs. [1] (solid points) and [15] (open points). Since the free NN scattering parameters are taken from [10], without adjustment, and a simple microscopic α particle wave function has been used, the only free parameter available was the assumed rms size of the α particle, through r_0. The level of agreement with the data for the physical rms matter radius of 1.49 fm is therefore very encouraging. No attempt was made to fine tune the NN interaction parameters. The experimental data also have a stated overall normalization uncertainty of order ± 2–3% [1,15].

B. Calculations for ^{6}He

For $p+^6$He scattering the dimensionality of the integrals involved in Eq. (11) is sufficiently small (five) that they are carried out directly by use of numerical quadratures. We require also $\mathcal{S}_4(b_\alpha)$, taken from the calculation above. For the ^{6}He three-body relative motion wave function, $\psi^{(3)}_{\rm rel}$, we took a representative selection of realistic (Faddeev) three-body wave function models from the family of models tabulated in Ref. [9]. The wave functions used were the P1, FC, and GB3 models which span a reasonably wide range of resulting ^{6}He rms matter radii. These yield ^{6}He radii of 2.33, 2.50, and 2.77 fm, respectively, when calculated assuming the α particle core radius is 1.49 fm, as used above.

Figure 3 shows the predicted $p+^6$He elastic differential cross sections resulting from the use of these three wave function models at 717 MeV. The figure shows that, while the elastic-scattering data are certainly consistent with the predictions of the FC model wave function, with a rms mat-

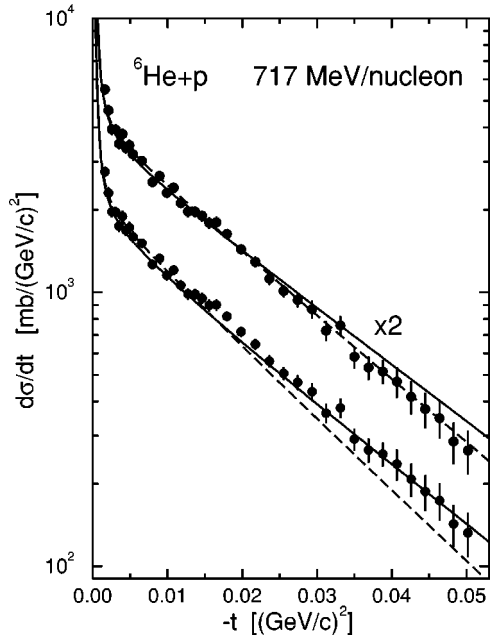

FIG. 4. Calculated and experimental $p+{}^6$He elastic differential cross section angular distribution at 717 MeV per nucleon. The solid curves reproduce the few-body results from Fig. 3 for ^{6}He rms radii of 2.33 fm (upper) and 2.50 fm (lower). The dashed curves show the results calculated for rms matter radii of 2.30 fm (upper) and 2.50 fm (lower) when using the density-based approximate description of Ref. [1].

ter radius of 2.50 fm, data of yet higher precision would be required to extract a precise value for the matter radius from such an analysis. The data are also subject to a small overall normalization uncertainty of $\pm 3\%$ [1]. We comment however that it was also the FC wave function which best reproduced the experimental ^{6}He$+{}^{12}$C total interaction cross section datum at 800 MeV/nucleon in a careful finite range study of that process [6]. The FC model is also the wave function which best reproduces the empirical ^{6}He three-body binding energy of 0.97 MeV.

We show, as an inset in Fig. 3, the calculated total reaction cross sections for the $p+{}^6$He system as a function of the ^{6}He rms matter radius for several wave-function models. These reveal a significant sensitivity to the projectile size and, if accessible experimentally, would provide a powerful constraint if used in combination with the angular distribution data.

In Fig. 4 we contrast the results of the analysis carried out here with those which result from the approximate (projectile density) approach followed by Alkhazov *et al.* [1,11]. In the figure, the solid curves are the same few-body results as in Fig. 3 for the wave functions with ^{6}He rms radii of 2.33 fm (upper) and 2.50 fm (lower). In these calculations the effects of the three-body correlations and of the use of ^{6}He wave functions with the correct three-body asymptotic behavior are included explicitly, as was discussed above. The dashed curves show the results calculated using the density-based method of Ref. [11] for the GH ^{6}He density of [1] with rms matter radii of 2.30 fm (upper) and 2.50 fm (lower) — that is when using the density-based approximate description. It is evident that the two approaches lead to quite different results. While the density-based calculations suggest that a radius of 2.50 fm is too large (manifest as too steep a gradient in the cross section versus q^2) and suggest a radius of 2.30 fm is appropriate [1], the more careful semimicroscopic treatment of the few-body aspects of the reaction, the solid curves, leads to the opposite conclusion.

C. Calculations for ^{8}He

For ^{8}He, calculation of $\mathcal{S}_8^{(5)}$ involves a 12-dimensional integration over the four chosen internal vector coordinates. The procedure used for ^{8}He was somewhat similar to that used for the ^{4}He, and used Monte Carlo sampling. At each ^{8}He c.m. impact parameter b, the position vectors $\boldsymbol{r}_i$ of the four nucleons relative to the α particle core were sampled and then $\langle|\psi_{\rm rel}^{(5)}(\boldsymbol{r}_1,\boldsymbol{r}_2,\boldsymbol{r}_3,\boldsymbol{r}_4)|^2\rangle_{\rm spin}$ of Eq. (13) was calculated. The position vectors $\boldsymbol{x}_\alpha=-\Sigma_{i=1}^4 m_n\boldsymbol{r}_i/(4m_n+m_\alpha)$ and $\boldsymbol{x}_i=\boldsymbol{r}_i+\boldsymbol{x}_\alpha$ of the α particle and the four neutrons relative to the projectile's c.m. could then be computed and hence the impact parameters of each constituent, b_j. In each such configuration the precalculated $S_n(b_i)$ and the $\mathcal{S}_4(b_\alpha)$, from the ^{4}He calculation above, were interpolated from a lookup table.

In the original COSMA wave function of Ref. [13] the valence neutron radial wave functions $\phi(r_i)$ entering Eq. (13) were assumed to be nodeless p-wave oscillator wave functions with a range parameter r_0, e.g., Eq. (2) of [13]. In the present work, for any given r_0, these oscillator radial functions are matched to a more correct p-wave Hankel function tail at the appropriate radius such that the radial function and its first derivative are continuous. As the two-neutron separation energy from ^{8}He is 2.137 MeV and the four-neutron separation energy is 3.1 MeV, we calculate the Hankel function tail assuming an average neutron separation energy of 1 MeV. Of course, in this case the wave function has to be renormalized to unity. Also, the simple relationship [13] between r_0, the rms matter radius of the ^{8}He and that of the ^{4}He core, $8\langle r^2\rangle_8-4\langle r^2\rangle_4=35r_0^2/4$, is now lost and the revised rms matter radius of ^{8}He for a given r_0 has to be computed numerically.

It is appreciated that this single-particle mean separation energy prescription for the valence nucleon wave function is only an approximation and that a more microscopic treatment of Φ_8 is desirable. It does however allow us to make a first assessment of the sensitivity of the calculations and of the data to our treatment of the wave-function asymptotics. The effect on the elastic scattering of going from an oscillator to a Hankel function tailed radial wavefunction is discussed below.

Figure 5 first shows the predicted and experimental $p+{}^8$He elastic differential cross section angular distribution at 674 MeV per nucleon. All of the calculations shown use the valence neutron radial wave function with the Hankel function tail and a neutron separation energy of 1 MeV. The curves correspond to wave functions with different r_0 and hence different ^{8}He rms matter radii as indicated. It is seen that wave functions with rms matter radii in the range 2.4–2.5 fm, as suggested by the density analysis of [1], do not reproduce the experimental data. The curve corresponding to a radius of 2.6 fm is consistent with the data within the few-body COSMA model used. We also show, as an inset in Fig. 5, the calculated total reaction cross sections for the p

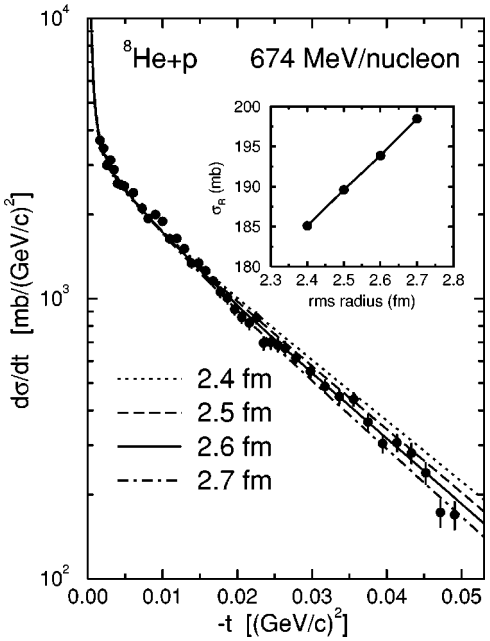

FIG. 5. Calculated and experimental $p+^8$He elastic differential cross section angular distribution as a function of the square of the four-momentum transfer ($q^2=-t$) at 674 MeV per nucleon. The calculations, all of which use a radial wave function with a Hankel function tail and n-separation energy 1 MeV, correspond to the different ^{8}He rms matter radii indicated. The inset shows the predicted total reaction cross sections as a function of the rms matter radius. The data are from Ref. [1].

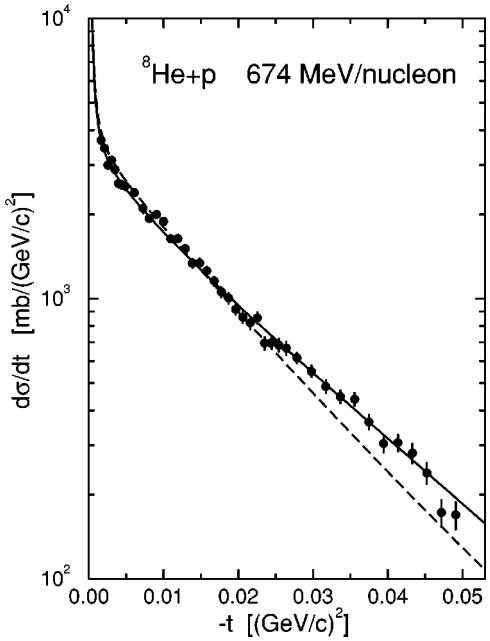

FIG. 6. Calculated and experimental $p+^8$He elastic differential cross section angular distribution at 674 MeV per nucleon. The solid curve shows the results using a radial wave function with a Hankel function tail and n-separation energy 1 MeV. The dashed curve results when using the oscillator model radial wave function. Both wave functions correspond to an rms matter radius for ^{8}He of 2.6 fm.

$+^8$He system as a function of the ^{8}He rms matter radius for the different wave functions. As for ^{6}He these reveal a significant sensitivity to the projectile size.

In Fig. 6 we investigate the sensitivity of the $p+^8$He calculations to the assumed asymptotics of the valence neutron single-particle state used in the COSMA model. The solid curve shows the results using the radial wave function with a Hankel function tail and a neutron separation energy of 1 MeV. The dashed curve results when using the original p-state oscillator model radial wave function for all radii. The two ^{8}He wave functions both correspond to the same rms matter radius for ^{8}He of 2.6 fm. We note the sensitivity of the calculated cross section to the wave-function asymptotics and conclude that a careful treatment of these few-body systems will be essential to making quantitative deductions from comparisons with such data.

In concluding this section we point out that the observed sensitivity to the wave-function asymptotics in the case of ^{8}He is also manifest in the case of ^{6}He. The differences we observe from the density-based calculations in Fig. 4, in the case of ^{6}He, stem from two sources. Namely, (1) the few-body cluster correlations in the wave function, and (2) our use of wave functions with *realistic three-body asymptotics*. When using simplified three-body models for ^{6}He, such as a $(p_{3/2})^2$ oscillator model, which includes the cluster structure of the projectile but without the correct asymptotics, calculated cross section curves in general fell between those of the density-based and exact few-body calculations. We warn therefore that the use of simplified few-body descriptions of the composite nuclei without the correct asymptotic behavior can lead to significant quantitative differences in predicted observables and hence in deduced spatial sizes.

IV. CONCLUDING REMARKS

We have presented a careful quantitative analysis of proton elastic scattering from the helium isotopes ^{4}He, ^{6}He, and ^{8}He at energies near 700 MeV/nucleon. We have formulated the elastic scattering in terms of Glauber theory and the few-body wavefunctions of the He nuclei. We have not made the additional approximations, which neglect few-body correlations, needed to reduce the dependence of the scattering upon the projectile structure simply to that of an assumed nuclear one-body density. We have shown that, as in the case of total reaction cross section calculations [8,9,6], an explicit treatment of these correlations in the few-body wave functions is of considerable quantitative importance.

We have used available three-body ($\alpha+2n$) and five-body ($\alpha+4n$) wave functions for ^{6}He and ^{8}He. Comparisons of the predicted cross sections with the recently reported data show that the deduced sizes of the He nuclei consistent with such an analysis are of order 0.2 fm larger than those deduced from the approximate procedure based on an assumed nuclear one-body density. With the model wave functions used, we observe that the data are consistent with few-body wave functions for ^{6}He and ^{8}He with matter radii of 2.50 and 2.60 fm, respectively, assuming an α particle core of radius 1.49 fm. This value for ^{6}He, larger than that for ^{6}Li, is consistent with values deduced from other empirical data [6,7].

We have also shown that there is significant sensitivity in the predicted cross sections to the asymptotic behavior of the wave functions used, both for ^{6}He and ^{8}He, and the increases in the deduced radii noted above stem from two sources. These are, (1) the intrinsic granular few-body nature of the wave functions, and (2) our use of wave functions, in

the case of ^{6}He, with realistic three-body asymptotics. The COSMA wave function used in the case of ^{8}He is probably too simple and certainly needs to be refined, but shows the same quantitative features. We conclude therefore that the use of simplified, e.g., Gaussian, few-body descriptions of the composite nuclei can lead to significant ambiguities in extracted spectroscopic information and also in the physical interpretation of data.

ACKNOWLEDGMENTS

The financial support of the Engineering and Physical Sciences Research Council (U.K.) through Grant No. GR/J95867 is gratefully acknowledged. The authors would like to thank Dr. S.R. Neumaier, IKP, Darmstadt, and Dr. P. Egelhof, GSI, Darmstadt, for providing the experimental data of the IKAR Collaboration in tabular form.

[1] G.D. Alkhazov *et al.*, Phys. Rev. Lett. **78**, 2313 (1997).
[2] R.J. Glauber, in *Lectures in Theoretical Physics*, edited by W.E. Brittin (Interscience, New York, 1959), Vol. 1, p. 315.
[3] H. de Vries, C. W. de Jager, and C. de Vries, At. Data Nucl. Data Tables **36**, 495 (1987).
[4] I. Tanihata, D. Hirata, T. Kobayashi, S. Shimoura, K. Sugimoto, and H. Toki, Phys. Lett. B **289**, 261 (1992).
[5] I. Tanihata *et al.*, Phys. Rev. Lett. **55**, 2676 (1985).
[6] J.A. Tostevin and J.S. Al-Khalili, Nucl. Phys. **A616**, 418c (1997).
[7] L.V. Chulkov, B.V. Danilin, V.D. Efros, A.A. Korshennnikov, and M.V. Zhukov, Europhys. Lett. **8**, 245 (1989).
[8] J.S. Al-Khalili and J.A. Tostevin, Phys. Rev. Lett. **76**, 3903 (1996).
[9] J.S. Al-Khalili, J.A. Tostevin, and I.J. Thompson, Phys. Rev. C **54**, 1843 (1996).
[10] L. Ray, Phys. Rev. C **20**, 1857 (1979).
[11] G.D. Alkhazov, S.L. Belostotsky, and A.A. Vorobyov, Phys. Rep., Phys. Lett. **42C**, 89 (1978).
[12] T. T. S. Kuo, F. Krmpotić, and Y. Tzeng, Phys. Rev. Lett. **78**, 2708 (1997).
[13] J.S. Al-Khalili, I.J. Thompson, and J.A. Tostevin, Nucl. Phys. **A581**, 331 (1995).
[14] M.V. Zhukov, A.A. Korsheninnikov, and M.H. Smedberg, Phys. Rev. C **50**, R1 (1994).
[15] O.G. Grebenjuk, A.V. Khanadeev, G.A. Korolev, S.I. Manayenkov, J. Saudinos, G.N. Velichko, and A.A. Vorobyov, Nucl. Phys. **A500**, 637 (1989).